



Three-dimensional echocardiography investigation of the mechanisms of tricuspid annular dilatation

Valentina Volpato^{1,2} · Victor Mor-Avi¹ · Federico Veronesi³ · Karima Addetia¹ · Megan Yamat¹ · Lynn Weinert¹ · Davide Genovese¹ · Gloria Tamborini² · Mauro Pepi² · Roberto M. Lang¹

Received: 9 April 2019 / Accepted: 7 August 2019 / Published online: 20 August 2019
© Springer Nature B.V. 2019

Abstract

Tricuspid annular (TA) size, assessed by 2D transthoracic echocardiography (TTE), has a well-established prognostic value in patients undergoing mitral valve surgery, with TA dilatation triggering simultaneous tricuspid annuloplasty. While TA dilatation is common in patients with dilated atria secondary to atrial fibrillation, little is known about the mechanisms of TA dilatation in patients with sinus rhythm (SR). This study aimed to identify echocardiographic parameters most closely related to the TA size as a potential tool for identification of patients prone to developing TA enlargement. 120 patients with SR underwent clinically indicated TTE, including 30 patients with normal hearts and 90 patients diagnosed with at least one right heart abnormality, defined as: right ventricular (RV) or right atrial (RA) dilatation, \geq moderate tricuspid regurgitation (TR) and elevated systolic pulmonary artery pressure (sPAP). RA and RV end-diastolic and end-systolic volumes (EDV, ESV) and function were measured using commercial 3D software (TomTec). 3D RV long and short axes were used as surrogate indices of RV shape. Degrees of TR and sPAP were estimated by 2D TTE. 3D TA sizing was performed at end-diastole using 3D custom software. Linear regression analysis was used to identify variables best correlated with TA size, followed by multivariate analysis to identify independent associations. The highest correlations were found between TA area and: RA ESV ($r=0.73$; $p<0.01$), RV EDV ($r=0.58$; $p<0.01$), RV end-diastolic long and short axes ($r=0.53, 0.42$; both $p<0.01$), TR degree ($r=0.40$; $p<0.01$) and sPAP ($r=0.32$; $p<0.01$). Multivariate analysis revealed that RA ESV was the only parameter independently associated with TA area ($p<0.05$, $r=0.85$). In conclusion, RA volume plays an important role in TA dilatation even in patients with normal SR. Understanding of annular remodeling mechanisms could aid in identifying patients at higher risk for TA dilatation, especially those scheduled for mitral valve surgery.

Keywords Tricuspid annulus · Tricuspid valve · 3D echocardiography · 3D volume · Right chambers

Abbreviations

EF	Ejection fraction	sPAP	Systolic pulmonary artery pressure
FAC	Fractional area change	3D	Three-dimensional
MR	Mitral regurgitation	TA	Tricuspid annular
MV	Mitral valve	TAPSE	Tricuspid annular plane systolic excursion
PISA	Proximal isovelocity surface area	TR	Tricuspid regurgitation
SR	Sinus rhythm	TV	Tricuspid valve
		2D	Two-dimensional
		RV	Right ventricular
		VC	Vena contracta

✉ Roberto M. Lang
rlang@medicine.bsd.uchicago.edu

¹ Section of Cardiology, Cardiac Imaging Center, University of Chicago Medical Center, 5758 S. Maryland Ave., MC 9067, Chicago, IL 60637, USA

² Department of Cardiovascular Imaging, Centro Cardiologico Monzino IRCCS, Milan, Italy

³ Department of Electrical, Electronics and Information Engineering, University of Bologna, Bologna, Italy

Introduction

Echocardiographic assessment of tricuspid annular (TA) dimensions should be standard practice in the evaluation of patients with mitral valve disease and severe mitral regurgitation (MR), who are considered for valve surgery [1, 2].

Recent studies showed that TA sizing may be important in patients undergoing percutaneous mitral valve (MV) repair, who may benefit from simultaneous tricuspid valve (TV) annuloplasty [3, 4]. Specifically, in patients with atrial fibrillation, atrial enlargement plays a predominant role in bilateral annular dilatation [5]. However, in patients with normal sinus rhythm (SR), the mechanisms of TA dilatation are not well understood, and accordingly, the ability to predict severe TA dilatation is limited. Per current guidelines, the presence of more than moderate tricuspid regurgitation (TR) in patients with severe MR identifies those at higher mortality risk [6–8], justifying concomitant tricuspid annuloplasty [1, 2, 9–11]. Moreover, in patients undergoing MV surgery, future development of significant TR as an epiphenomenon of TA dilatation [12], has led to considering isolated annular enlargement as an indication for simultaneous TV repair, as recommended by current guidelines [1].

Despite the fact that simultaneous tricuspid annuloplasty improves functional TR parameters, data regarding long-term mortality are inconsistent [13, 14]. However, previous studies have shown that with adequate patient selection [1], the strategy of routine tricuspid annuloplasty significantly reduces TR, contributing to beneficial long-term right heart remodeling [13]. Nevertheless, at the time of left valve surgery, the number of patients eligible for simultaneous TV repair ranges between 6 and 60% [13], underscoring that in these patients, right heart remodeling may have already occurred [15]. Importantly, despite repair of the left sided valvular abnormality, TA remodeling is a dynamic process that is usually not alleviated by isolated treatment of the mitral valve disease [16]. Nowadays there is insufficient data regarding the selection of patients suitable for tricuspid repair at the time of MV surgery, in whom right heart remodeling has already occurred [17, 18]. Identification of these patients may be helpful for mitigating the risk for TA dilatation and subsequent TR development. However, this requires better understanding of the mechanisms of TA enlargement.

Echocardiographic assessment of the TA plays a crucial role in patients excluded from simultaneous tricuspid annuloplasty. Current TA measurements rely on two-dimensional (2D) transthoracic echocardiography (TTE) [1, 2], which is intrinsically limited by its view dependency, resulting in underestimation of annular dimensions when compared to three-dimensional (3D) assessment [19, 20]. Moreover, 2D echocardiographic TA measurements have higher inter-observer variability, often making the follow-up of TA dimensions equivocal [21]. Methodology-related underestimation of TA dimensions is a known pitfall in annular measurements and also a confounding factor in the evaluation of the mechanisms of TA enlargement. Recent studies suggest that these limitations may be easier to overcome with the use of 3D echocardiography [21]. Accordingly, the aim of

this study was to identify 3D echocardiographic parameters most closely related to TA dimensions, as a potential tool for early identification of patients with higher probability of impending annular enlargement.

Methods

This retrospective study included 128 patients, referred for clinically indicated TTE at two institutions, the University of Chicago Medical Center (Chicago, Illinois, USA) and the Cardiologic Center Monzino (Milan, Italy) between June 2017 and June 2018. Enrolment criteria were based on echocardiographic diagnosis of normal heart or primary or secondary right-heart disease, with at least one right-heart abnormality. Patients were excluded if they had cardiac arrhythmias, pacemakers, previous cardiac surgery, congenital heart disease or poor endocardial border visualization, which was defined as the lack of visualization of 3 contiguous segments using a 17-segment model of the left ventricle, as well as incomplete visualization of the right ventricular (RV) free wall and both atria. Thus, only 3D datasets in which TA boundaries could be traced with confidence by an experienced investigator and accurately detected by semi-automated software, were used. According to current guidelines [1, 22], right heart abnormalities were defined on 2D and 3D [20, 22–25] images as: RV dilatation and/or dysfunction, RA dilatation, \geq moderate tricuspid regurgitation and elevated systolic pulmonary artery pressure (sPAP). The Institutional Review Boards of both Institutions approved the study, and informed consent was obtained from each patient. Analysis was performed at the University of Chicago Medical Center.

A comprehensive 2D echocardiographic examination was performed using a commercial ultrasound system (i33 or Epiq7, Philips Healthcare, Andover, MA) equipped with an X5-1 probe. After optimization of 2D images by adjusting the depth, gain and time-gain compensation, 3D full-volume datasets of right heart chambers were obtained from the RV-focused apical 4-chambers view using electrocardiographic gating over two consecutive cardiac cycles during held end-expiration. The frame rate of the 3D datasets was optimized by adjusting the elevation and sector width.

First, right heart chambers' linear dimensions were assessed on 2D images, using the RV-focused apical 4-chambers view. The single-plane disks summation method was used for RA volume determination at end-systole; whereas end-diastolic and end-systolic indexed areas were used for the assessment of RV size. According to current recommendations [22], RA enlargement using 2D imaging was defined as a volume > 27 and 32 ml/m² for female and male patients, respectively. Using 3D imaging, RA volumes of > 38 and 49 ml/m² for females and males,

respectively, were used as cutoffs for enlargement [20]. RV systolic function was assessed using fractional area change (FAC), tricuspid annular plane systolic excursion (TAPSE) on M-Mode images and S' -wave velocity by tissue Doppler imaging [22]. According to guidelines [22], RV dilation was defined as RV end-diastolic indexed area > 11.5 or $12.6 \text{ cm}^2/\text{m}^2$ for females and males, respectively. RV dysfunction was defined as TAPSE $< 17 \text{ mm}$ or S' -wave velocity $< 9.5 \text{ cm/s}$ or FAC $< 35\%$ for 2D. RV dysfunction using 3D was defined as an RV ejection fraction (EF) $< 45\%$. SPAP and TR degree were assessed as recommended by current guidelines [1, 2]; elevated sPAP was defined as values $> 37 \text{ mmHg}$ [22]. TR degree was quantified based on the dimensions of the vena contracta (VC) and the dimension of the radius of the regurgitant jet using the proximal isovelocity surface area (PISA) method in either the RV inflow, apical 4-chamber or the RV-focused apical 4-chamber views. For TR classification, the echocardiographic view showing the largest VC dimensions or PISA radius was chosen. The hepatic vein flow by pulsed-wave Doppler in the subcostal view was also used, when available, for better classification of TR. TR severity was graded as: 0 = absent, 1 = trivial, 2 = mild, 3 = mild to moderate, 4 = moderate, 5 = moderate to severe, 6 = severe [1, 2].

Thereafter, 3D analysis was performed offline using commercial software (TomTec, Unterschleissheim, Germany). End-diastolic and end-systolic RV volumes were obtained using semi-automated software (TomTec 4D RV-Analysis)

(Fig. 1). End-diastolic and end-systolic RA volumes were obtained using the LV analysis algorithm (TomTec 4D LV-Analysis) adapted for 3D atrial measurements, as previously described [23] (Fig. 2). The 3D atrial and ventricular EFs were then calculated. Moreover, RV analysis also provided measurements of 3D end-diastolic long and basal axes, that were used as surrogate measures of RV shape. RV free-wall and septal peak-systolic strains were also assessed using semi-automated software for RV analysis (Fig. 1).

Finally, 3D TA measurements, including area, perimeter and long axis, were performed using previously described custom software [24] at end-diastole, defined as the frame just prior to TV leaflet closure. Briefly, the software allows 3D reconstruction of the annulus along all three spatial dimensions. After manual orientation of orthogonal and cross-sectional planes to optimize TV visualization, the software exports a 3D full-volume dataset into Cartesian coordinates. The 3D dataset is then used to extract several 2D planes, containing the TV, each one rotated around the RA-RV direction. The software automatically detects the TV insertion points (hinge points) on each 2D plane, allowing a complete 3D reconstruction of the annular geometry. Manual correction of the hinge points was performed as needed, depending on the quality of the 3D dataset (Fig. 3).

Since there are no guidelines-recommended 3D cutoff values for the diagnosis of TA enlargement, normal annular dimensions were defined based on the largest available study that reported annular dimensions in normal volunteers

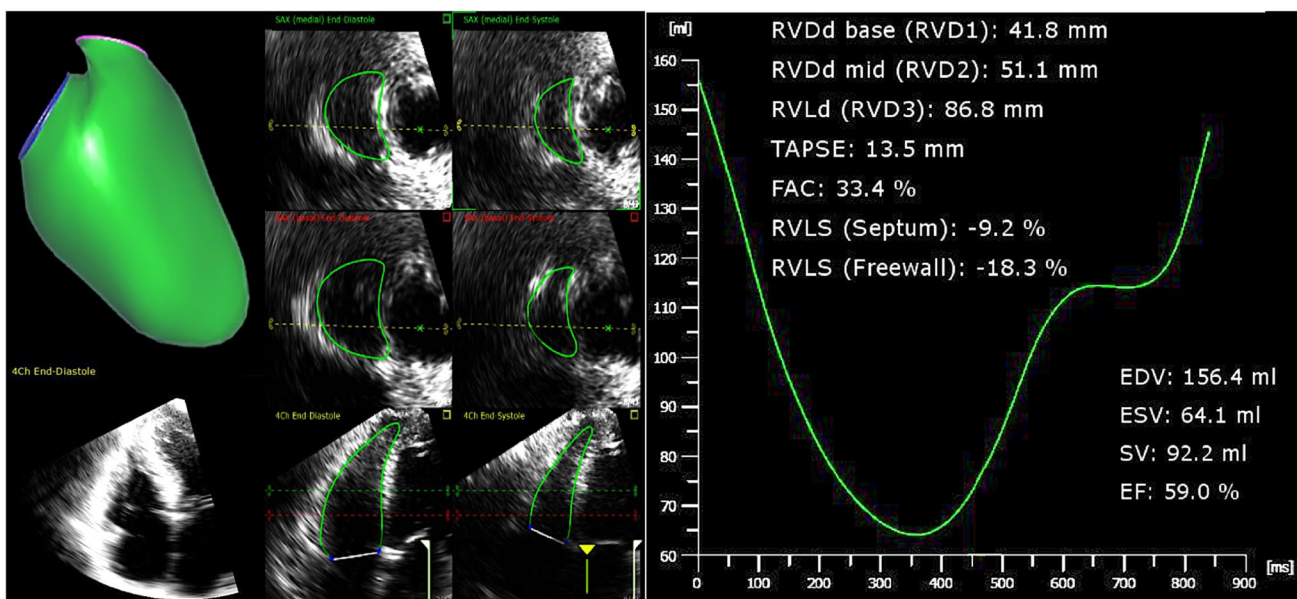


Fig. 1 3D right ventricular assessment using commercial software for right ventricular analysis. Ventricular endocardium is detected at end-diastole and end-systole, verified by the reader using long- and short-axis views to obtain right ventricular 3D reconstruction (on the left). Time-volume curve of the right ventricle is automatically gener-

ated by the software, as well as chamber volumes and function (on the right). *EVD* end-diastolic volume, *EDVi* end-diastolic volume indexed, *ESV* end systolic volume, *ESVi* end systolic volume indexed, *SV* stroke volume, *EF* ejection fraction

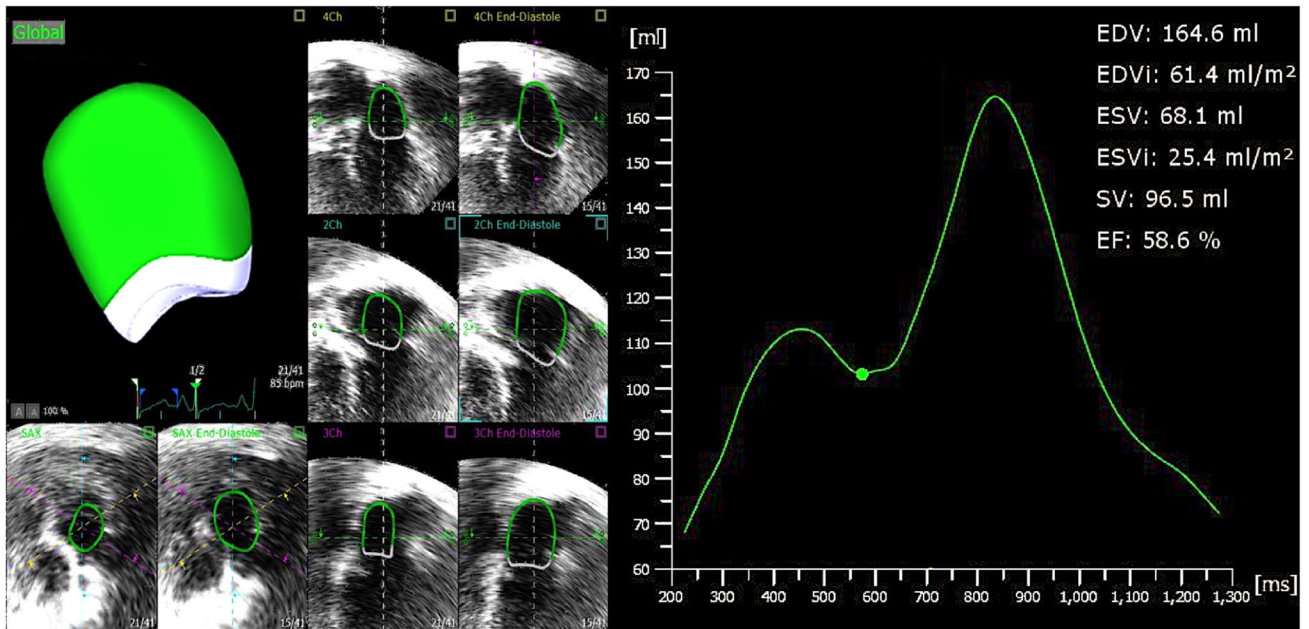


Fig. 2 3D right atrial assessment using commercial software for left ventricular analysis, adjusted for atrial measurements. Atrial boundaries are detected at ventricular end-diastole (end-systolic frame for the atrium) and ventricular end-systole (end-diastolic frame for the atrium). Tracking of atrial borders can be verified by the reader using long- and short-axis views to obtain right atrial 3D reconstruction

(on the left). Time-volume curve of the right atrium is automatically generated by the software, as well as chamber volumes and function (on the right). *EDV* end-diastolic volume, *EDVi* end-diastolic volume indexed, *ESV* end systolic volume, *ESVi* end systolic volume indexed, *SV* stroke volume, *EF* ejection fraction

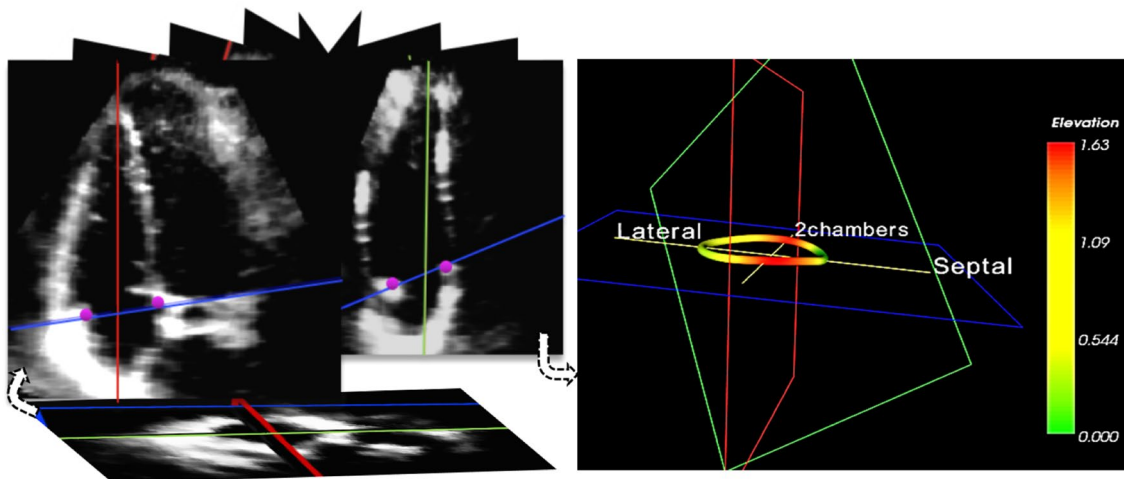


Fig. 3 3D tricuspid annular assessment using custom software for tricuspid valve analysis. The 3D dataset (bottom left) is automatically divided by the software into several 2D planes rotating around the z-plane (top left). On each plane, the software identifies the annular hinge points, each of one is defined by a specific x–y–z coordinate (purple circles on the top left); hinge points can be manually cor-

rected by the reader. A blue plane, crossing each hinge points and containing the annulus, is automatically generated and it allows the 3D reconstruction of the annular structure. On the right, the 3D annulus is depicted from a 2 chambers view, showing annular spatial orientation (interventricular septal-right ventricular lateral wall orientation); the annular height is represented using a color-code map

[24]. Indexed axes, perimeter and area were used to evaluate the normality of annular size in male and female subjects. The annulus was defined as normal when at least three

dimensions among indexed long axis, short axis, perimeter and area were within the normal ranges [24].

Table 1 Baseline and right heart characteristics of study population

Baseline characteristics	
Population (N)	120
Male (%)	48
Age (years)	59 ± 19
Height (cm)	168 ± 14
Weight (Kg)	79 ± 25
BSA (m ²)	2 ± 0
Heart rate (bpm)	80 ± 17
Systolic blood pressure (mmHg)	135 ± 22
Diastolic blood pressure (mmHg)	77 ± 14
Right heart characteristics	
RV dilation (N)	59
RV dysfunction (N)	31
RA dilation (N)	37
Elevated sPAP (N)	61
≥ moderate TR (N)	32
Normal heart	30

RV right ventricle, RA right atrium, sPAP systolic pulmonary artery pressure, TR tricuspid regurgitation

Statistical analysis

Statistical analysis was performed using SPSS software (SPSS Inc., Chicago, IL, USA). Continuous variables are presented as mean ± SD. Categorical data are presented as percentages or absolute numbers. Linear regression analysis with Pearson's correlation was used to identify echocardiographic variables that correlated best with TA dimensions. 3D end-diastolic TA area, perimeter and long axis were correlated to each of the following 3D dependent variables: end-diastolic and end-systolic RA volumes, RA EF, end-diastolic and end-systolic RV volumes, RV EF, RV long and basal axes, RV free wall strain, RV septal strain. Moreover, linear regression was performed between end-diastolic annular area, perimeter and long axis and sPAP, as well as degree of TR. Same analyses were repeated using indexed TA dimensions (area, perimeter and long axis) and indexed right-chambers volume and axes (end-diastolic and end-systolic RA and RV volumes, RV long and basal axes). Variables showing the highest correlations ($r > 0.30$) with

statistical confidence ($p < 0.01$) with TA dimensions were selected for the multivariate analysis, which was used to identify independent associations among the selected variables. A pre-test analysis of variance (F-statistic, $< 5\%$) was performed to test the null hypothesis.

Results

After excluding 8 patients from the initial cohort of 128, due to poor 3D image quality, the final study group consisted of 120 patients. This included 30 patients with normal hearts and 90 patients diagnosed with at least one right heart abnormality. The baseline characteristics of study subjects are presented in Table 1. The average frame rate of 3D images was 26 ± 11 Hz. Manual correction of TA hinge points was required in the majority of patients ($n = 108, 90\%$).

Among patients with right heart disorders, 78 (87%) had secondary and 12 (13%) primary right heart disease due to pulmonary arterial hypertension. These patients were categorized as shown in Table 2. The echocardiographic characteristics of the study subjects are shown in Table 3. Based on previous data, 77 patients (64%) could be determined to have normal gender-related 3D TA dimensions, including 32 (67%) males and 45 (62%) females [24].

When compared to annular perimeter and long axis, end-diastolic TA area showed the best correlation with the majority of the echocardiographic variables. Subsequently, end-diastolic TA area was chosen as the independent variable. To avoid collinearity on multivariate analysis, only the RV end-diastolic (maximal) volume and the RA end-systolic (maximal) volume were entered into the multivariate model; both variables showed higher correlations with TA area compared to RV end-systolic and RA end-diastolic volumes.

Results of univariate regression analyses are presented in Table 4. Linear regression analysis showed an appreciable association between RV end-diastolic volume and TA area, perimeter and long axis, with the highest correlation noted between RV volume and TA area ($r = 0.58, p < 0.001$; Fig. 4, top left). Correlation coefficients between RV systolic function and TA dimensions (area, perimeter and area) were low; this also included RV free-wall and septal strain. Analysis

Table 2 Patient classification into categories based on main disease. Right chambers dilatation was defined when at least one chamber dilatation (either right ventricle or atrium) was noted

Right heart chambers	Right ventricular function	Tricuspid regurgitation	Systolic pulmonary artery pressure	N	%
Dilated	Reduced	≥ Moderate	Elevated	41	34.0
Dilated	Reduced	< Moderate	Elevated	15	12.5
Dilated	Reduced	< Moderate	Normal	21	17.5
Normal	Normal	< Moderate	Elevated	13	11.0
Normal	Normal	None	Normal	30	25.0

Table 3 2D and 3D echocardiographic characteristics of study population.

Echocardiographic characteristics		
2D echocardiography	Standard	Indexed (/m ²)
Dimensions		
LV BP end-diastolic volume (ml)	123 ± 64	65.1 ± 30.7
LV BP end-systolic volume (ml)	62.6 ± 54	32.9 ± 27.5
LA BP volume (ml)	70.2 ± 34	37.1 ± 17.9
RV end-diastolic area (cm ²)	26.8 ± 8.7	14.3 ± 4.27
RV end-systolic area (cm ²)	15.5 ± 7.5	8.25 ± 3.73
RA volume (ml)	58.4 ± 32	31.2 ± 17.7
Function		
LV BP EF (%)	54.1 ± 16	
RV FAC (%)	44.1 ± 11	
RV TAPSE (mm)	20.9 ± 7	
RV S' TDI (cm/s)	13.2 ± 3.9	
Valve disease		
MR ≥ moderate (N)	36	
MS ≥ moderate (N)	2	
AR ≥ moderate (N)	10	
AS ≥ moderate (N)	3	
TR ≥ moderate (N)	32	
TR Vena Contracta (mm)	5.65 ± 1.9	
TR PISA radius (mm)	7.53 ± 2.5	
TS (N)	0	
Pulmonary pressure		
sPAP (mmHg)	44.3 ± 17	
3D echocardiography	Standard	Indexed (/m ²)
Dimensions		
RV end-diastolic volume (ml)	155 ± 59	82.2 ± 28.4
RV end-systolic volume (ml)	78.3 ± 43	41.6 ± 22
RV basal diameter (cm)	3.57 ± 0.7	1.93 ± 0.45
RV long axis (cm)	8.67 ± 1.1	4.69 ± 0.72
RA end-systolic volume (ml)	62.8 ± 28	33.6 ± 14.6
RA end-diastolic volume (ml)	28.4 ± 17	15.1 ± 8.84
Function		
RV EF (%)	51.5 ± 11	
RV free wall strain (%)	− 25 ± 6.7	
RV septal strain (%)	− 13 ± 5.4	
RA EF (%)	55.8 ± 10	
Tricuspid annulus		
TA long axis (cm)	4.34 ± 0.7	2.35 ± 0.49
TA short axis (cm)	3.54 ± 0.7	1.91 ± 0.45
TA perimeter (cm)	12.5 ± 2.1	6.75 ± 1.43
TA area (cm ²)	12.3 ± 4.1	6.63 ± 2.37

See text for details

BP biplane (using disk-summation method), *LV* left ventricle, *LA* left atrium, *RV* right ventricle, *RA* right atrium, *EF* ejection fraction, *FAC* fractional area change, *TAPSE* tricuspid annular plane systolic excursion, *TDI* tissue Doppler imaging, *MR* mitral regurgitation, *MS* mitral stenosis, *AR* aortic regurgitation, *AS* aortic stenosis, *TR* tricuspid regurgitation, *PISA* proximal isovelocity surface area, *TS* tricuspid stenosis; *sPAP* systolic pulmonary arterial pressure, *TA* tricuspid annulus

Table 4 Results of linear regression analyses between 3D tricuspid annular dimensions and echocardiographic variables

Echocardiographic variables	Tricuspid annulus						p
	Long axis (cm)	Long axis (cm/m ²)	Perimeter (cm)	Perimeter (cm/m ²)	Area (cm ²)	Area (cm ² /m ²)	
RV end-diastolic volume (ml)	0.55		0.56		0.58		< 0.0001
RV end-diastolic volume (ml/m ²)		0.45		0.46		0.56	< 0.0001
RV end-systolic volume (ml)	0.52		0.52		0.55		< 0.0001
RV end-systolic volume (ml/m ²)		0.41		0.42		0.51	< 0.0001
RV EF (%)	− 0.40	− 0.23	− 0.38	− 0.23	− 0.40	− 0.33	< 0.0001
RV basal diameter (cm)	0.40		0.42		0.42		< 0.0001
RV basal diameter (cm/m ²)		0.52		0.53		0.43	< 0.0001
RV long axis (cm)	0.49		0.52		0.53		< 0.0001
RV long axis (cm/m ²)		0.69		0.69		0.56	< 0.0001
RV free wall strain (%)	0.41		0.38		0.38		< 0.0001
RV septal strain (%)	0.29		0.28		0.28		< 0.0001
RA end-systolic volume (ml)	0.67		0.70		0.73		< 0.0001
RA end-systolic volume (ml/m ²)		0.69		0.54		0.73	< 0.0001
RA end-diastolic volume (ml)	0.65		0.68		0.71		< 0.0001
RA end-diastolic volume (ml/m ²)		0.54		0.57		0.68	< 0.0001
RA EF (%)	− 0.41	− 0.24	− 0.42	− 0.25	− 0.42	− 0.34	< 0.0001
TR degree	0.40	0.35	0.37	0.34	0.40	0.38	< 0.0001
sPAP (mmHg)	0.33	0.26	0.33	0.27	0.32	0.30	< 0.0001

Results are presented as correlation coefficients (r), $p < 0.01$ indicated statistical significance. Analyses between variables were performed using both absolute values and indexed values

RV right ventricle, EF ejection fraction, RA right atrium, TR tricuspid regurgitation, sPAP systolic pulmonary artery pressure

of RV long and basal axes showed an association between these variables and TA area (Fig. 4, top right and middle left, respectively), perimeter and long axis; correlations were slightly higher when TA area was used ($r = 0.53$, $p < 0.001$ for long axis; $r = 0.42$, $p < 0.001$ for basal axis).

RA end-systolic (maximal) and end-diastolic volumes correlated well with TA dimensions, with the highest correlation noted between RA end-systolic volume and TA area ($r = 0.73$, $p < 0.001$; Fig. 4, middle right). The correlations between the degree of TR and the three TA dimensions were weaker ($r = 0.40$, $p < 0.001$ for both TA area and long axis) (Fig. 4, bottom left). Similarly, the degree of sPAP and TA dimensions revealed a low correlation between these parameters ($r < 0.4$, $p < 0.001$ for TA area, perimeter and long axis) (Fig. 4, bottom right).

Linear regression analyses between each of the TA indexed dimensions (area, perimeter and long axis) and indexed RV volume, RA volume and RV axes showed the same trend as noted with the non-indexed variables

(Table 4), while for the non-indexed variables, the correlations were lower than between indexed echocardiographic variables and TA indexed area, compared to indexed TA perimeter and axis.

Multivariate analysis (Table 5, bottom) showed that only RA end-systolic volume was independently associated with TA end-diastolic area ($p < 0.001$). In contrast, neither RV end-diastolic volume nor RV axes, degree of TR and sPAP were independently associated with TA size ($p > 0.05$).

Discussion

In this study, we investigated the echocardiographic variables associated with the 3D TA dimensions enlargement in a heterogeneous cohort of patients with normal SR. Our results showed that patients with larger TA areas have larger RA volumes, suggesting that atrial enlargement may be a

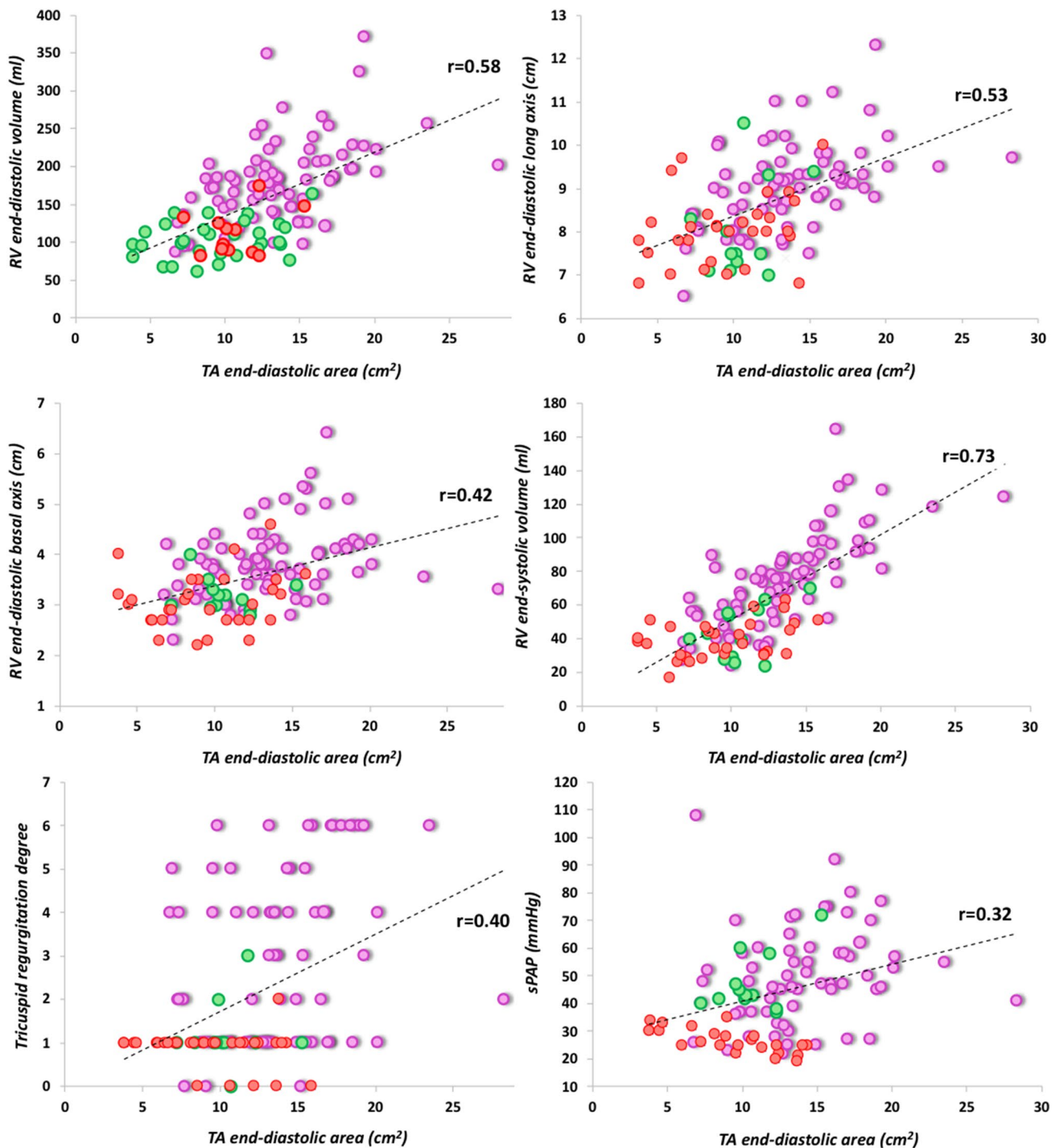


Fig. 4 Echocardiographic variables showing the highest correlation with tricuspid annular end-diastolic area (biggest annular area in cm^2), based on the results of simple linear regression analyses ($p < 0.001$). Different subgroups are shown in different colors: red and

purple—primary and secondary right heart disease, respectively, and green—normal hearts. *TA* tricuspid annulus, *RV* right ventricle, *RA* right atrium, *sPAP* systolic pulmonary artery pressure

critical factor in annular dilatation even in patients without atrial fibrillation.

Despite the role of TA enlargement in the development of TR, few data are available regarding the mechanisms of

TA dilatation [16]. It has been shown that both RA and TA enlargement appear to be triggered by severe TR, but no data is available regarding the synergistic role of right-heart chamber volumes, TR severity and pulmonary pressure

Table 5 Pre-test analysis of variance using F-statistic (<5%) allowing to reject the null hypothesis (top)

ANOVA								
Model	Sum of squares		df	Mean square		F	p	
Regression	1,042,207		6	173,701		22,473	0.000	
Residual	718,815		93	7,729				
Total	1,761,022		99					
Model	Non-standardized B coefficient	Std. error	Standardized B coefficient	t	p	95% CI for B coefficients		Collinearity
						Lower limit	Upper limit	
(Constant)	2.097	3.107		0.675	0.502	– 4.074	8.267	
RV ED vol	0.010	0.009	0.151	1.192	0.236	– 0.007	0.028	0.237
RV long axis	0.361	0.448	0.094	0.807	0.442	– 0.528	1.250	0.321
RV basal axis	0.025	0.488	0.004	0.051	0.960	– 0.944	0.994	0.599
RA ES vol	0.080	0.013	0.558	6.119	0.000	0.054	0.106	0.528
sPAP	0.000	0.022	– 0.001	– 0.100	0.992	– 0.043	0.043	0.545
TR	0.191	0.196	0.860	0.971	0.334	– 0.199	0.581	0.558

Results of multivariate model (bottom, $R=0.769$) showing that RA end-systolic volume was the only independent variable associated with tricuspid annular end-diastolic area

Dependent Variable: TA Area

ED end-diastolic, ES end-systolic, RV right ventricle, RA right atrium, sPAP systolic pulmonary artery pressure, TR tricuspid regurgitation

in TA remodeling [25]. In patients with atrial fibrillation, the predominant role of RA volume in determining annular dimensions has been demonstrated previously [5]. Our results underline the dependency of TA enlargement on RA size, also in patients with SR. Surprisingly, RV volumes and RV long-axis dimension, used as surrogate indices of RV shape, seem to play a secondary role in modulating TA dimensions.

In our study group, 31 patients (26%) were diagnosed with moderate to severe TR, but TR severity did not strongly correlate with TA enlargement. The progression of TR is associated with different pathophysiological mechanisms [26, 27]; particularly, TR is a continuum of two main mechanisms. On one hand, TR could be related to leaflet tethering without significant annular enlargement, a common finding in patients with pulmonary hypertension [28]. On the other hand, TR may be the result of significant annular dilatation without TV leaflet involvement, as can be found in patients with atrial fibrillation [12]. To further complicate matters, the development of TR may over time result in RA dilatation, and, as a consequence, TR may contribute towards progressive TA enlargement that worsens regurgitation. Finally, TR degree is also strongly dependent on the hemodynamic status of the patient, based on loading conditions. In our study, TR severity was not independently associated with TA dimension. This may be due to the wide spectrum of mechanisms contributing to TR development and explaining the fact that patients with significant TR do not necessarily have dilated TA and vice-versa. Thus, it seems that TR may contribute to TA dilatation via RA enlargement, which

results in aggravation of annular dilatation and TR degree in a sort of feedback loop reaction.

Surprisingly, in our study, RV volumes appeared not to be significantly related to TA dimensions. This may be due to the fact that patients enrolled in our study had different pathologies which affected RV volumes and geometry differently. Thus, RV remodeling may be different among patients, depending on the underlying disease, making the annular size to be influenced by the ventricle based on the type and degree of RV remodeling. Only patients in whom the RV remodeling predominantly affects the medio-basal segments may develop a significant annular dilatation determined by the ventricle rather than the atrium. This may explain the fact that, similar to the TR degree, in our multivariate model, RV volumes and axes were not independently associated with TA dimensions.

Understanding the mechanisms of TA dilatation may be of particular importance based on the well-established prognostic role played by annular dimensions in patients undergoing MV surgery [9]. Previous data showed that TR progression after isolated MV surgery is closely related to annular dilatation [29]. However, at the time of MV repair, the eligibility of patients for simultaneous tricuspid annuloplasty is based on a 'single' static evaluation of 2D TA dimensions. Since TA remodeling is a dynamic process, identification of patients at higher risk of future TA enlargement after left-heart surgery, may be helpful in the management of this subgroup of patients.

The presence of RA enlargement in patients with SR undergoing MV surgery could potentially be used as a

predictor of possible TA dilatation and TR development, highlighting the need for a closer echocardiographic and clinical follow-up of these patients. In fact, based on the established high mortality risk of TV surgery after isolated left-sided valvular repair, current guidelines recommend that treatment of late secondary severe TR be performed earlier, particularly if signs of progressive RV dilatation or dysfunction are present, even in asymptomatic patients [1]. Early identification of these patients is crucial, thus the presence of echocardiographic predictors for TA dilatation may trigger a different post-surgical management in this population.

Another interesting point is the recurrence of significant TR after annuloplasty, that is diagnosed in 8–15% of patients after MV surgery [30, 31]. Our study did not investigate the role of RA volume in these patients, however, further studies are needed to identify which parameters are closely related to TA repair failure.

Limitations

Our study was retrospective in nature and the study group was relatively small. Another limitation is the heterogeneity of our population, including a wide variety of different diseases involving the right heart. To circumvent this limitation, we categorized patients into different classes based on the underlying diseases, however the percentage of patients in each category was not equal. TA dimensions were measured using custom software, which is not universally available.

Conclusions

RA volume plays an important role in TA dilatation, irrespective of the presence of atrial fibrillation. The understanding of annular remodeling mechanisms could be of particular importance in identifying patients with higher probability of TA dilatation whose annular dimensions are crucial at the time of surgical decision-making prior to mitral valve surgery. Particularly, among patients in sinus rhythm undergoing isolated MV repair, the presence of RA enlargement may highlight a subgroup of patients at higher risk of TA enlargement, underscoring the potential need for close post-surgical echocardiographic follow-up.

Compliance with ethical standards

Conflict of interest The authors declare that they have no competing interest.

Ethical approval All procedures performed in studies involving human participants were in accordance with the ethical standards of the insti-

tutional and/or national research committee and with the 1964 Helsinki declaration and its later amendments or comparable ethical standards.

Informed consent The study was approved by the Institutional Review Board with a waiver of consent.

References

- Baumgartner H, Falk V, Bax JJ et al (2017) 2017 ESC/EACTS guidelines for the management of valvular heart disease. *Eur Heart J* 38:2739–2791
- Nishimura RA, Otto CM, Bonow RO et al (2017) 2017 AHA/ACC focused update of the 2014 AHA/ACC guideline for the management of patients with valvular heart disease: a report of the American College of Cardiology/American Heart Association Task Force on Clinical Practice Guidelines. *J Am Coll Cardiol* 70:252–289
- Asmarats L, Puri R, Latib A et al (2018) Transcatheter tricuspid valve interventions: landscape, challenges, and future directions. *J Am Coll Cardiol* 71:2935–2956
- Hausleiter J, Braun D, Orban M et al (2018) Patient selection, echocardiographic screening and treatment strategies for interventional tricuspid repair using the edge-to-edge repair technique. *EuroIntervention* 14:645–653
- Utsunomiya H, Itabashi Y, Mihara H et al (2017) Functional tricuspid regurgitation caused by chronic atrial Fibrillation: a real-time 3-dimensional transesophageal echocardiography study. *Circ Cardiovasc Imaging* 10:e004897
- Nath J, Foster E, Heidenreich PA (2004) Impact of tricuspid regurgitation on long-term survival. *J Am Coll Cardiol* 43:405–409
- Koelling TM, Aaronson KD, Cody RJ et al (2002) Prognostic significance of mitral regurgitation and tricuspid regurgitation in patients with left ventricular systolic dysfunction. *Am Heart J* 144:524–529
- Topilsky Y, Nkomo VT, Vatury O et al (2014) Clinical outcome of isolated tricuspid regurgitation. *JACC Cardiovasc Imaging* 7:1185–1194
- Benedetto U, Melina G, Angeloni E et al (2012) Prophylactic tricuspid annuloplasty in patients with dilated tricuspid annulus undergoing mitral valve surgery. *J Thorac Cardiovasc Surg* 143:632–638
- Dreyfus GD, Corbi PJ, Chan KM et al (2005) Secondary tricuspid regurgitation or dilatation: which should be the criteria for surgical repair? *Ann Thorac Surg* 79:127–132
- Van de Veire NR, Braun J, Delgado V et al (2011) Tricuspid annuloplasty prevents right ventricular dilatation and progression of tricuspid regurgitation in patients with tricuspid annular dilatation undergoing mitral valve repair. *J Thorac Cardiovasc Surg* 141:1431–1439
- Shiran A, Sagie A (2009) Tricuspid regurgitation in mitral valve disease incidence, prognostic implications, mechanism, and management. *J Am Coll Cardiol* 53:401–408
- Chikwe J, Itagaki S, Anyanwu A et al (2015) Impact of concomitant tricuspid annuloplasty on tricuspid regurgitation, right ventricular function, and pulmonary artery hypertension after repair of mitral valve prolapse. *J Am Coll Cardiol* 65:1931–1938
- Pettinari M, De Kerchove L, Lazam S et al (2018) Mid-term results of a randomized trial of tricuspid annuloplasty for less-than-severe functional tricuspid regurgitation at the time of mitral valve surgery†. *Eur J Cardiothorac Surg* 55(5):851–858

15. Seeburger J, Borger MA, Falk V et al (2008) Minimal invasive mitral valve repair for mitral regurgitation: results of 1339 consecutive patients. *Eur J Cardiothorac Surg* 34:760–765
16. Fukuda S, Saracino G, Matsumura Y et al (2006) Three-dimensional geometry of the tricuspid annulus in healthy subjects and in patients with functional tricuspid regurgitation: a real-time, 3-dimensional echocardiographic study. *Circulation* 114:I492–I498
17. Duran CM, Pomar JL, Colman T et al (1980) Is tricuspid valve repair necessary? *J Thorac Cardiovasc Surg* 80:849–860
18. Kara I, Koksali C, Erkin A et al (2015) Outcomes of mild to moderate functional tricuspid regurgitation in patients undergoing mitral valve operations: a meta-analysis of 2488 patients. *Ann Thorac Surg* 100:2398–2407
19. Miglioranza MH, Mihăilă S, Muraru D et al (2015) Variability of tricuspid annulus diameter measurement in healthy volunteers. *JACC Cardiovasc Imaging* 8:864–866
20. Miglioranza MH, Mihăilă S, Muraru D et al (2015) Dynamic changes in tricuspid annular diameter measurement in relation to the echocardiographic view and timing during the cardiac cycle. *J Am Soc Echocardiogr* 28:226–235
21. Volpato V, Lang RM, Yamat M et al (2019) Echocardiographic assessment of the tricuspid annulus: the effects of the third dimension and measurement methodology. *J Am Soc Echocardiogr* 32(2):238–247
22. Lang RM, Badano LP, Mor-Avi V et al (2015) Recommendations for cardiac chamber quantification by echocardiography in adults: an update from the American Society of Echocardiography and the European Association of Cardiovascular Imaging. *J Am Soc Echocardiogr* 28(1–39):e14
23. Tamborini G, Fusini L, Muratori M et al (2016) Right heart chamber geometry and tricuspid annulus morphology in patients undergoing mitral valve repair with and without tricuspid valve annuloplasty. *Int J Cardiovasc Imaging* 32:885–894
24. Addetia K, Muraru D, Veronesi F, et al. (2019) 3-Dimensional echocardiographic analysis of the tricuspid annulus provides new insights into tricuspid valve geometry and dynamics. *J Am Coll Cardiol Cardiovasc Img* 12:401–412. <https://doi.org/10.1016/j.jcmg.2017.08.022>
25. Nemoto N, Schwartz JG, Lesser JR et al (2017) The right atrium and tricuspid annulus are cardinal structures in tricuspid regurgitation with or without pulmonary hypertension. *Int J Cardiol* 230:171–174
26. Nemoto N, Lesser JR, Pedersen WR et al (2015) Pathogenic structural heart changes in early tricuspid regurgitation. *J Thorac Cardiovasc Surg* 150:323–330
27. Buzzatti N, De Bonis M, Moat N (2018) Anatomy of the tricuspid valve, pathophysiology of functional tricuspid regurgitation, and implications for percutaneous therapies. *Interv Cardiol Clin* 7:1–11
28. Medvedofsky D, Aronson D, Gomberg-Maitland M et al (2017) Tricuspid regurgitation progression and regression in pulmonary arterial hypertension: implications for right ventricular and tricuspid valve apparatus geometry and patients outcome. *Eur Heart J Cardiovasc Imaging* 18:86–94
29. Izumi C, Miyake M, Takahashi S et al (2011) Progression of isolated tricuspid regurgitation late after left-sided valve surgery. Clinical features and mechanisms. *Circ J* 75:2902–2907
30. Navia JL, Nowicki ER, Blackstone EH et al (2010) Surgical management of secondary tricuspid valve regurgitation: annulus, commissure, or leaflet procedure? *J Thorac Cardiovasc Surg* 139(1473–82):e5
31. McCarthy PM, Bhudia SK, Rajeswaran J et al (2004) Tricuspid valve repair: durability and risk factors for failure. *J Thorac Cardiovasc Surg* 127:674–685

Publisher's Note Springer Nature remains neutral with regard to jurisdictional claims in published maps and institutional affiliations.